Progress In Electromagnetics Research M, Vol. 114, 59–67, 2022

Robust Slow Light Enhancement Based on Flat Band States in the Continuum

Yanhong Liu[1, *], Kai Sun[1], Mina Ren[2], Lijuan Dong[1], Fusheng Deng[1], Xiaoqiang Su[1], and Yunlong Shi[1]

Abstract—Flat band systems have attracted considerable interest in different branches of physics, providing a flexible platform for exploring the fundamental properties of flat bands. Flat band states in the continuum (FBICs) can be derived from a one-dimensional lattice loaded with electromagnetically induced transparency (EIT) medium. The appearance of the strong slow light phenomena has been found under the conditions of EIT and flat band. Flat bands provide a key ingredient in designing dispersionless wave excitations. Different from the conventional flat band states, the FBIC is delocalized state and has robustness, providing us an efficient way to achieve large delay slow light. These results may provide inspiration for exploring fundamental phenomena arising from FBICs.

1. INTRODUCTION

In recent years, there has been a surge of interest for the physics in flat band system [1–19]. It is well known that the motion of an electron in a periodic lattice can be described by Bloch theory, and its band structure is usually composed of dispersion curves. However, the conventional wisdom has been defied by the surprising discovery of the flat band (FB) [20], a dispersion-free energy band characterized by a group velocity of zero for the wave packet throughout the Brillouin region. These novel properties of flat band physics have attracted a great deal of theoretical and experimental interest in a variety of fields, including ultracold atoms [5, 21–25], various metamaterials [26–29], exciton-polariton condensates [22, 30–32], photonic waveguide arrays [4, 11, 33–36], and more. People have realized the flat band by constructing some special lattice structures with "geometrical frustration" [37], strengthening the magnetic field [38, 39], constructing strain structures [40–43], introducing twist angles [44–47], etc. A lot of researches have been carried out on the novel physical phenomena brought about by them.

Electromagnetic induced transparency (EIT), which is originally rooted in quantum physics system, has been widely used in the research of slow lights [48–52], sensors [53–55], absorbers [56–58], optical modulators [59, 60], nonlinear enhancement [61, 62], and other fields, due to its slow wave effect, strong dispersion, low absorption, and high-quality factor spectrum response. The analogue of EIT effect based on microwave metamaterials [52, 63–65], in particular, provides a new platform for the observation of slow wave effect, which not only is easy to adjust in structure, but also can visually reveal the strong dispersion effect caused by the EIT phenomenon. So far, the studies of the EIT structure are all focused on the transmission characteristics and group delay, while the in-depth investigation on energy band characteristics of periodic structures composed of EIT mediums and dielectric remains lacking. To the best of our knowledge, it is the first time that a special FB located in the passband is proposed, which

Received 21 August 2022, Accepted 14 October 2022, Scheduled 18 October 2022
* Corresponding author: Yanhong Liu (lyh030114@163.com).
[1] Shanxi Province key Laboratory of Microstructure Electromagnetic Functional Materials, Shanxi Datong University, Datong 037009, Shanxi, China. [2] Key Laboratory of Advanced Micro-structure Materials, MOE, School of Physics Science and Engineering, Tongji University, Shanghai 200092, China.

is different from the conventional FB in band gap opened at the boundary or the central of the Brillouin zone.

In this work, we will combine the concepts of the flat band and EIT effect in a photonic crystal composed of dielectric and EIT medium to explore the possibility of enhancing the robust slow light phenomena. In Section 2, the equivalent photonic crystal model for studying FBIC is introduced and analyzed, including EIT metamaterial and waveguide configuration, then the band structure of multilayer system is calculated for firstly using hybrid theory based on coupled mode method (CMM) and transfer matrix method (TMM). In Section 3, We present the numerical results of the designed finite EIT lattice structures to realize FBIC. The transmission spectrum and group delay are in agreement with the predictions of hybrid theory. Furthermore, we show that FBIC is robust to loss, providing solid evidence for the stability of the slow-light phenomenon. Finally, a brief conclusion and prospect are presented in Sec. 4.

2. THEORETICAL MODEL

In this section, we analyze the band structure of a lattice composed of alternating layers, which consist of alternating arrangements of EIT metamaterial and waveguide structures, as shown in Figure 1. In the illustrated model, slow wave effect can be easily observed and exploited at room temperature. EIT in metamaterials replaces three-level atoms with artificial atoms and replaces the interference between microscopic quantum channels with the interference between macroscopic light fields. Sun et al. [52] have experimentally observed the dynamic evolution of EIT in a waveguide system. Similar to the structure in [52], we consider the EIT realized in metamaterials with a waveguide configuration, as shown in Figure 1(a), and the open-ended comb line ($l = 15\,\text{mm}$, $w = 0.2\,\text{mm}$) can be considered as a bright resonator. SRRs formed by two edge-coupled split rings ($g = 0.2\,\text{mm}$, $a = 6.4\,\text{mm}$) can be considered as a dark resonator.

Our theoretical investigation begins with TMM, which allows one to obtain the band structure (ω versus k), reflection coefficient, and transmission with the help of Bloch theory [66]. Figure 1(c) shows

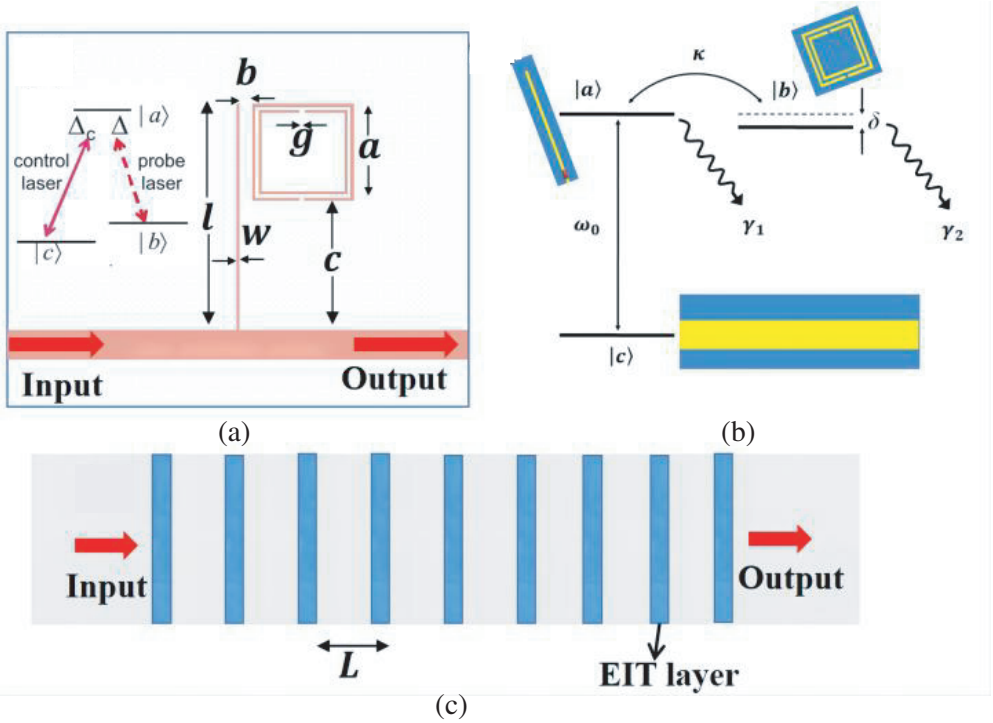

Figure 1. (Color online) (a) Photograph of the EIT medium, (b) Analogy diagram of a metamaterial and three level atomic system, (c) lattice composed of finite number of alternating EIT and dielectric layers.

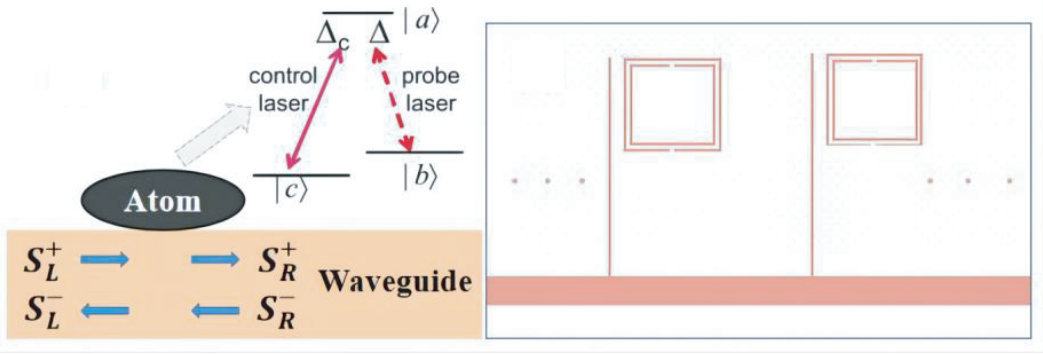

(a) (b)

Figure 2. (Color online) (a) The scheme of the atomic level structure and (b) the 1D super lattice made of a backbone waveguide and EIT.

the one-dimensional lattice loaded with EIT elements, and L is the lattice constant. The electric field on every position $[E(x)]$ can be decomposed into forward wave $[E_+(x)]$ and backward wave $[E_-(x)]$, which meets the condition $E(x) = E_+(x) + E_-(x)$. The electric fields on different positions are connected by the transfer matrix. First, we build a model of interaction of photons with the three-level atom, as shown in Figure 2(a). Combining TMM and CMM, a hybrid theory to calculate the band structure is presented. Similar to the transfer matrix method joined with coupled-mode theory in [52], the transfer matrix for the EIT medium can be written as:

$$M_{EIT} = \frac{1}{t}\begin{pmatrix} 1 & -r_L \\ r_R & t^2 - r_L r_R \end{pmatrix}, \tag{1}$$

with the transmission coefficient of EIT medium $t = 1 - \frac{\gamma_1[i(\omega-\omega_2)+\Gamma_2]}{[i(\omega-\omega_1)+\gamma_1+\Gamma_1][i(\omega-\omega_2)+\Gamma_2]+\kappa^2}$ and reflection coefficient of EIT medium $r_L = r_R = -\frac{\gamma_1[i(\omega-\omega_2)+\Gamma_2]}{[i(\omega-\omega_1)+\gamma_1+\Gamma_1][i(\omega-\omega_2)+\Gamma_2]+\kappa^2}$, where κ is the coupling coefficient; ω_1 and ω_2 are resonance frequency of the comb line and SRRs, respectively; γ_1 is the spontaneous emission attrition rate of the bright resonator; Γ_1 and Γ_2 are the intrinsic loss of bright and dark resonators, respectively.

The transfer matrix for an entire unit cell in Figure 2(b) connects the electric field on two sides of the unit cell by

$$\begin{pmatrix} E_{m+1}^+ \\ E_{m+1}^- \end{pmatrix} = M \begin{pmatrix} E_m^+ \\ E_m^- \end{pmatrix}, \tag{2}$$

where the transfer matrix for lattice unit cell can be written as $M = M_D M_{EIT} M_D$. The transfer matrix M_D for the backbone waveguide (homogeneous medium) can be written as:

$$M_D = \begin{pmatrix} e^{jkL/2} & 0 \\ 0 & e^{-jkL/2} \end{pmatrix}. \tag{3}$$

Then, for a finite structure with N unit cells, the total transfer matrix can be obtained from the product of a transfer matrix for the single unit cell $M^{(N)} = M^N$, in which

$$M = \frac{1}{t}\begin{pmatrix} e^{-i\cdot kL} & -r_L \\ r_R & \left(t^2 - r_L r_R\right)\cdot e^{i\cdot kL} \end{pmatrix}. \tag{4}$$

According to the Born-Karman boundary condition, we have

$$\begin{pmatrix} E_{m+1}^+ \\ E_{m+1}^- \end{pmatrix} = e^{jqa} \begin{pmatrix} E_m^+ \\ E_m^- \end{pmatrix}. \tag{5}$$

where q is the Bloch wave vector, and L is the length of the unit cell. From Equations (2) and (5), we can get

$$M \begin{pmatrix} E_m^+ \\ E_m^- \end{pmatrix} = e^{jqa} \begin{pmatrix} E_m^+ \\ E_m^- \end{pmatrix}. \tag{6}$$

The band structure of EIT lattice shown in Figure 1(c) can be obtained from the transfer matrix of the single unit cell combined with Bloch boundary conditions $\cos(qL) = \frac{M_{11}+M_{22}}{2}$, namely,

$$\cos(qL) = \left[1 - \frac{\gamma_1 \left[i\left(\omega - \omega_2\right) + \Gamma_2\right]}{\left[i\left(\omega - \omega_1\right) + \gamma_1 + \Gamma_1\right]\left[i\left(\omega - \omega_2\right) + \Gamma_2\right] + \kappa^2}\right] \cos\left(kL\right) \tag{7}$$

Corresponding band structures are calculated as shown in Figure 3. Here, the parameters are consistent with those in [52], $L = 15\,\text{mm}$, $\gamma_1 = 0.38\,\text{GHz}$, $f_1 = \omega_1/2\pi = 3.74\,\text{GHz}$, $f_2 = \omega_2/2\pi = 3.69\,\text{GH}$, $\kappa = 0.318\,\text{GH}$, $\Gamma_1 = \Gamma_2 = 0$. The frequency ranges from 3.64 GHz to 3.74 GHz in the band structure correspond to FBIC.

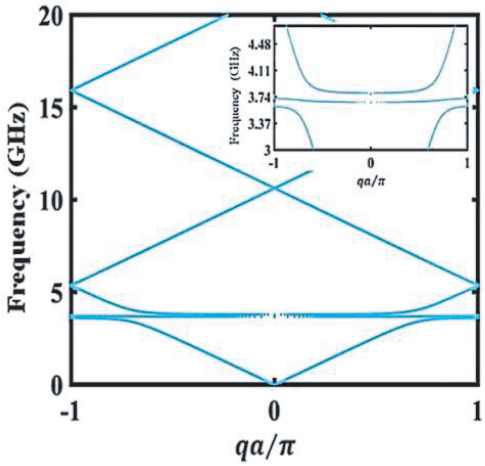

Figure 3. Band structures for 1D EIT lattice.

3. NUMERICAL RESULTS AND DISCUSSION

In order to validate our analytical calculations and further elucidate the slow light response of the EIT lattice, we numerically calculate the transmission spectra and group delay of the finite EIT lattice structures using CST Microwave Studio. The transmission and group delay spectra of the EIT element are plotted in Figure 4. A transmission window emerges with a peak transmittance exceeding 90% at 3.7 GHz. So, what are the effects resulting from the 1D EIT lattice? A conventional one-dimensional PC,

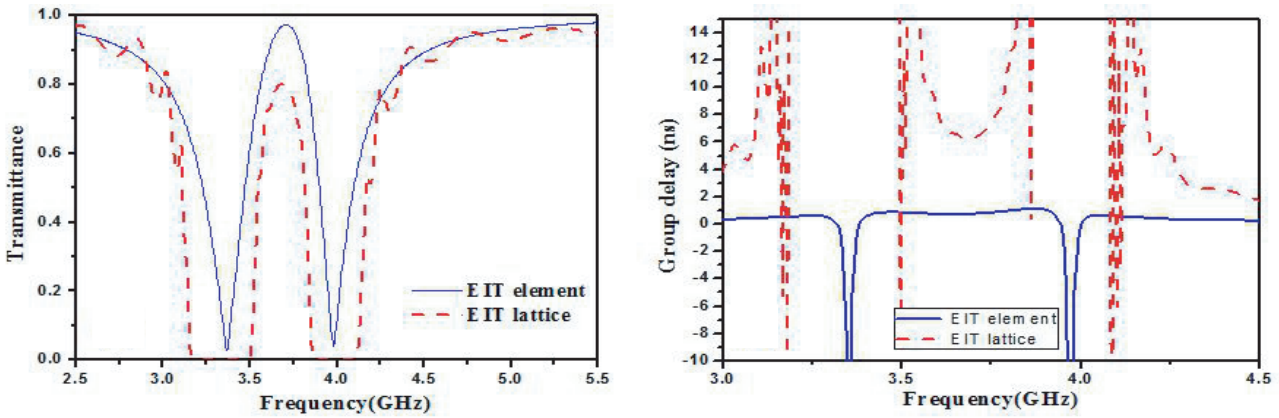

Figure 4. (Color online) (a) Simulated transmittances and (b) group delay of the EIT element and EIT lattice, respectively.

$(AB)^N$, where N is the periodic number, and the lattice constant $L = d_{AB} = 15\,\text{mm}$ was considered. A and B denote the EIT and homogeneous dielectric, respectively. The transmission spectra of truncated PC $(AB)^9$ are presented in Figure 4(a). It provides extra degrees of freedom for controlling the spectra through the structural element and lattice constants. Zhang et al. [67] realized slow light with ultra-flat dispersion in hybrid photonic crystal waveguide. We investigate the slow-wave effect, and the simulated results of group delay time are shown in Figure 4(b). A transmission window emerges in frequency ranges from 3.64 GHz to 3.74 GHz with a peak transmittance exceeding 75%. The group delay time in the FBIC of EIT lattice has reached 6.26 ns, while the group delay time of EIT element is 0.78 ns. Therefore, we realized slow light with FBIC.

We then investigate the influence of the loss on the transmittance and slow wave effect. An adjustable resistance $R \leq 20\,\Omega$ is inserted into the junction, which is a tunable intrinsic loss in the EIT element. The transmission spectra, field distributions, and group delay time with different R are shown in Figure 5. From Figure 5(b), we can find that the field distribution is non-localized, and fields are distributed in the dark resonator, so the transmittance and group delay time are nearly R independent. It has also been predicted that the FBIC features are robust.

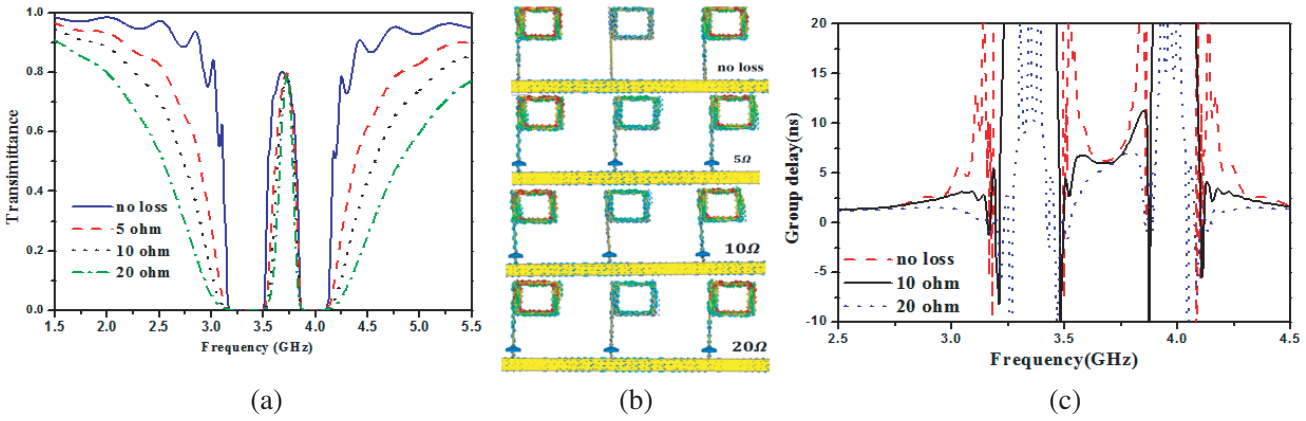

Figure 5. (Color online) (a) Simulated transmittances of the EIT lattice vs R, (b) numerical surface current distributions, (c) group delay of the EIT lattice vs R.

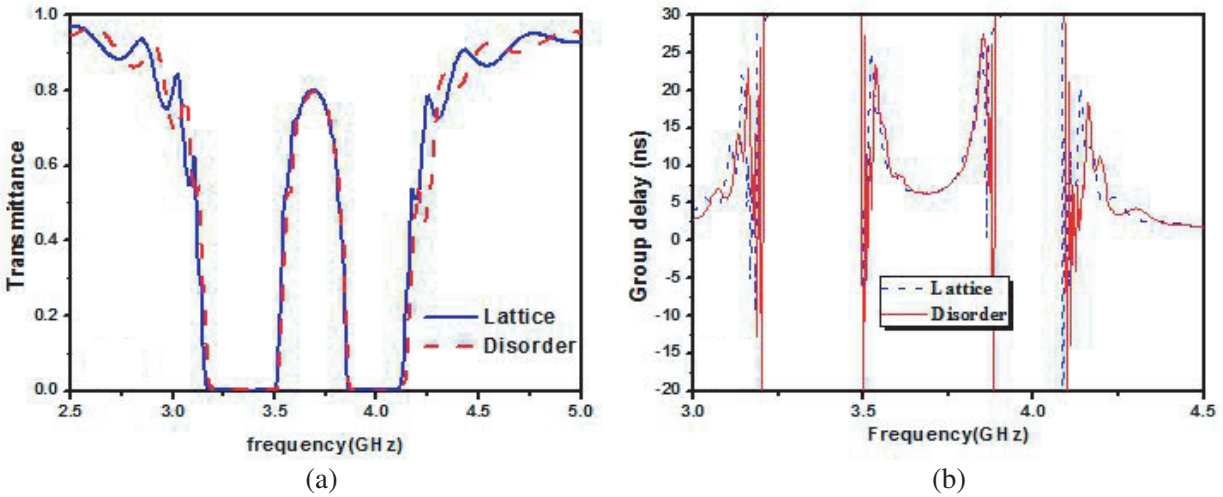

Figure 6. (Color online) (a) Transmission coefficient spectrum of the EIT lattice. The blue line corresponds to the lattice, that is, lattice constant is 15 mm, and the red line corresponds to the disorder, that is, distances between element are 14 mm, 15 mm, 14 mm, 13.5 mm, 14 mm, 15 mm, 13 mm, 13.5 mm, respectively. (b) The group delay of the EIT lattice.

For traditional flat band, the vanishing transverse group velocity allows the lattice to support compact eigenstates that are perfectly localized at several lattice sites, with exactly vanishing amplitude in all other sites. As a result, the periodicity was changed even slightly, and the propagating mode can be destroyed. When we destroy the periodicity of the EIT lattice, the slow light is robust, because the FBIC is non-localized. From Figure 6, we can find that the transmittance and group delay time are changed little, when the distance between lattice elements was changed from 15 mm to 14 mm, 15 mm, 14 mm, 13.5 mm, 14 mm, 15 mm, 13 mm, 13.5 mm.

4. CONCLUSION

In summary, we present a novel method to generate robust slow light effect using an EIT lattice with flat dispersion. The results of the numerical simulations indicate that non-localization of flat band in the EIT lattices shows that the flat band is in non-localized states. We have studied the transmission and slow-light behavior in an EIT element and EIT lattice. Under the EIT and FBIC condition, we realized larger delay slow light with FBIC. Under the non-localization of FBIC condition, the maximum transmittance as well as the corresponding group delay is nearly unchanged with intrinsic loss in a bright resonator and disorder. Therefore, our results provide novel ideas for future studies in FBIC, and they highlight the importance of non-localization flat band systems.

ACKNOWLEDGMENT

This work was supported by the Natural National Science Foundation of China (NSFC) under Grant 11874245, and 61805129, the Central Government guides local science and Technology Development Fund projects under Grant YDZJSX2021B011 and YDZJSX2021C032, Key Research and Development Program of Shanxi Province, China under Grant Nos. 201903D121071 and 201903D121026.

REFERENCES

1. White, S. and L. Sham, "Electronic properties of flat-band semiconductor heterostructures," *Physical Review Letters*, Vol. 47, 879, 1981.
2. Bergholtz, E. J. and Z. Liu, "Topological flat band models and fractional Chern insulators," *International Journal of Modern Physics B*, Vol. 27, 1330017, 2013.
3. Derzhko, O., J. Richter, and M. Maksymenko, "Strongly correlated flat-band systems: The route from Heisenberg spins to Hubbard electrons," *International Journal of Modern Physics B*, Vol. 29, 1530007, 2015.
4. Mukherjee, S., A. Spracklen, D. Choudhury, et al., "Observation of a localized flat-band state in a photonic Lieb lattice," *Physical Review Letters*, Vol. 114, 245504, 2015.
5. Mukherjee, S. and R. R. Thomson, "Observation of localized flat-band modes in a quasi-one-dimensional photonic rhombic lattice," *Optics Letters*, Vol. 40, 5443–5446, 2015.
6. Zong, Y., S. Xia, L. Tang, et al., "Observation of localized flat-band states in Kagome photonic lattices," *Optics Express*, Vol. 24, 8877–8885, 2016.
7. Leykam, D., S. Flach, and Y. Chong, "Flat bands in lattices with non-Hermitian coupling," *Physical Review B*, Vol. 96, 064305, 2017.
8. Leykam, D., A. Andreanov, and S. Flach, "Artificial flat band systems: From lattice models to experiments," *Advances in Physics: X*, Vol. 3, 1473052, 2018.
9. Longhi, S., "Photonic flat-band laser," *Optics Letters*, Vol. 44, 287–290, 2019.
10. Xia, S.-Q., L.-Q. Tang, S.-Q. Xia, et al., "Novel phenomena in flatband photonic structures: From localized states to real-space topology," *Acta Physica Sinica*, Vol. 69, No. 15, 154207, 2020.
11. Tang, L., D. Song, S. Xia, et al., "Photonic flat-band lattices and unconventional light localization," *Nanophotonics*, Vol. 9, 1161–1176, 2020.
12. Maimaiti, W., A. Andreanov, and S. Flach, "Flat-band generator in two dimensions," *Physical Review B*, Vol. 103, 165116, 2021.

13. Poblete, R. A. V., "Photonic flat band dynamics," *Advances in Physics: X*, Vol. 6, No. 1, 1878057, 2021.
14. Han, C.-D. and Y.-C. Lai, "Optical response of two-dimensional Dirac materials with a flat band," *Physical Review B*, Vol. 105, 155405, 2022.
15. Hanafi, H., P. Menz, and C. Denz, "Localized states emerging from singular and nonsingular flat bands in a frustrated fractal-like photonic lattice," *Advanced Optical Materials*, Vol. 10, 2102523, 2022.
16. Hanafi, H., P. Menz, A. McWilliam, et al., "Localized dynamics arising from multiple flat bands in a decorated photonic Lieb lattice," arXiv e-prints, 2022, arXiv: 2207.01480.
17. Li, G., L. Wang, R. Ye, et al., "Observation of flat-band and band transition in the synthetic space," *Advanced Photonics*, Vol. 4, 036002, 2022.
18. Shen, Y.-X., Y.-G. Peng, P.-C. Cao, et al., "Observing localization and delocalization of the flat-band states in an acoustic cubic lattice," *Physical Review B*, Vol. 105, 104102, 2022.
19. Zhang, R.-H., H.-Y. Ren, and L. He, "Flat bands and related novel quantum states in two-dimensional systems," *Acta Physica Sinica*, Vol. 71, 127302–127301, 2022.
20. Sutherland, B., "Localization of electronic wave functions due to local topology," *Physical Review B*, Vol. 34, 5208, 1986.
21. Vicencio, R. A., C. Cantillano, L. Morales-Inostroza, et al., "Observation of localized states in Lieb photonic lattices," *Physical Review Letters*, Vol. 114, 245503, 2015.
22. Masumoto, N., N. Y. Kim, T. Byrnes, et al., "Exciton-polariton condensates with flat bands in a two-dimensional kagome lattice," *New Journal of Physics*, Vol. 14, 065002, 2012.
23. Shen, R., L. Shao, B. Wang, et al., "Single Dirac cone with a flat band touching on line-centered-square optical lattices," *Physical Review B*, Vol. 81, 041410, 2010.
24. Taie, S., H. Ozawa, T. Ichinose, et al., "Coherent driving and freezing of bosonic matter wave in an optical Lieb lattice," *Science Advances*, Vol. 1, e1500854, 2015.
25. Baboux, F., L. Ge, T. Jacqmin, et al., "Bosonic condensation and disorder-induced localization in a flat band," *Physical Review Letters*, Vol. 116, 066402, 2016.
26. He, S., F. Ding, L. Mo, et al., "Light absorber with an ultra-broad flat band based on multi-sized slow-wave hyperbolic metamaterial thin-films," *Progress In Electromagnetics Research*, Vol. 147, 69–79, 2014.
27. Lazarides, N. and G. Tsironis, "SQUID metamaterials on a Lieb lattice: From flat-band to nonlinear localization," *Physical Review B*, Vol. 96, 054305, 2017.
28. Lazarides, N. and G. Tsironis, "Compact localized states in engineered flat-band $\mathcal{PT}$ metamaterials," *Scientific Reports*, Vol. 9, 1–9, 2019.
29. Qian, K., L. Zhu, K. H. Ahn, et al., "Observation of flat frequency bands at open edges and antiphase boundary seams in topological mechanical metamaterials," *Physical Review Letters*, Vol. 125, 225501, 2020.
30. Sun, M., I. Savenko, S. Flach, et al., "Excitation of localized condensates in the flat band of the exciton-polariton Lieb lattice," *Physical Review B*, Vol. 98, 161204, 2018.
31. Scafirimuto, F., D. Urbonas, M. A. Becker, et al., "Tunable exciton-polariton condensation in a two-dimensional Lieb lattice at room temperature," *Communications Physics*, Vol. 4, 1–6, 2021.
32. Klembt, S., T. H. Harder, O. A. Egorov, et al., "Polariton condensation in S- and P-flatbands in a two-dimensional Lieb lattice," *Applied Physics Letters*, Vol. 111, 231102, 2017.
33. Li, J., T. P. White, L. O'Faolain, et al., "Systematic design of flat band slow light in photonic crystal waveguides," *Optics Express*, Vol. 16, 6227–6232, 2008.
34. Vicencio Poblete, R. A., "Photonic flat band dynamics," *Advances in Physics: X*, Vol. 6, 1878057, 2021.
35. Hou, J., D. Gao, H. Wu, et al., "Flat band slow light in symmetric line defect photonic crystal waveguides," *IEEE Photonics Technology Letters*, Vol. 21, 1571–1573, 2009.
36. Endo, S., T. Oka, and H. Aoki, "Tight-binding photonic bands in metallophotonic waveguide networks and flat bands in kagome lattices," *Physical Review B*, Vol. 81, 113104, 2010.

37. Bergman, D. L., C. Wu, and L. Balents, "Band touching from real-space topology in frustrated hopping models," *Physical Review B*, Vol. 78, 125104, 2008.
38. Peres, N., F. Guinea, and A. C. Neto, "Electronic properties of disordered two-dimensional carbon," *Physical Review B*, Vol. 73, 125411, 2006.
39. Peres, N., A. C. Neto, and F. Guinea, "Conductance quantization in mesoscopic graphene," *Physical Review B*, Vol. 73, 195411, 2006.
40. Guinea, F., M. Katsnelson, and A. Geim, "Energy gaps and a zero-field quantum Hall effect in graphene by strain engineering," *Nature Physics*, Vol. 6, 30–33, 2010.
41. Levy, N., S. Burke, K. Meaker, et al., "Strain-induced pseudo–magnetic fields greater than 300 tesla in graphene nanobubbles," *Science*, Vol. 329, 544–547, 2010.
42. Rechtsman, M. C., J. M. Zeuner, A. Tünermann, et al., "Strain-induced pseudomagnetic field and photonic Landau levels in dielectric structures," *Nature Photonics*, Vol. 7, 153–158, 2013.
43. Wen, X., C. Qiu, Y. Qi, et al., "Acoustic Landau quantization and quantum-Hall-like edge states," *Nature Physics*, Vol. 15, 352–356, 2019.
44. Yin, L.-J., J.-B. Qiao, W.-J. Zuo, et al., "Experimental evidence for non-Abelian gauge potentials in twisted graphene bilayers," *Physical Review B*, Vol. 92, 081406, 2015.
45. Cao, Y., V. Fatemi, A. Demir, et al., "Correlated insulator behaviour at half-filling in magic-angle graphene superlattices," *Nature*, Vol. 556, 80–84, 2018.
46. Hao, Z., A. Zimmerman, P. Ledwith, et al., "Electric field-tunable superconductivity in alternating-twist magic-angle trilayer graphene," *Science*, Vol. 371, 1133–1138, 2021.
47. Shen, C., Y. Chu, Q. Wu, et al., "Correlated states in twisted double bilayer graphene," *Nature Physics*, Vol. 16, 520–525, 2020.
48. Amin, M., R. Ramzan, and O. Siddiqui, "Slow wave applications of electromagnetically induced transparency in microstrip resonator," *Scientific Reports*, Vol. 8, 2357, 2018.
49. Zeng, A. W. and B. Guo, "Characteristics of slow light in a magnetized plasma hyperbolic metamaterial waveguide," *Optical and Quantum Electronics*, Vol. 49, 200, 2017.
50. Keshavarz, A. and A. Zakery, "A novel terahertz semiconductor metamaterial for slow light device and dual-band modulator applications," *Plasmonics*, Vol. 13, 459–466, 2018.
51. Lee, M.-J., J. Ruseckas, C.-Y. Lee, et al., "Experimental demonstration of spinor slow light," *Nature Communications*, Vol. 5, 5542, 2014.
52. Sun, Y., H. Jiang, Y. Yang, et al., "Electromagnetically induced transparency in metamaterials: Influence of intrinsic loss and dynamic evolution," *Physical Review B*, Vol. 83, 195140, 2011.
53. Liu, N., T. Weiss, M. Mesch, et al., "Planar metamaterial analogue of electromagnetically induced transparency for plasmonic sensing," *Nano Letters*, Vol. 10, 1103–1107, 2010.
54. Alipour, A., A. Farmani, and A. Mir, "High sensitivity and tunable nanoscale sensor based on plasmon-induced transparency in plasmonic metasurface," *IEEE Sensors Journal*, Vol. 18, 7047–7054, 2018.
55. Hayashi, S., D. V. Nesterenko, and Z. Sekkat, "Waveguide-coupled surface plasmon resonance sensor structures: Fano lineshape engineering for ultrahigh-resolution sensing," *Journal of Physics D: Applied Physics*, Vol. 48, 325303, 2015.
56. Tassin, P., L. Zhang, R. Zhao, et al., "Electromagnetically induced transparency and absorption in metamaterials: The radiating two-oscillator model and its experimental confirmation," *Physical Review Letters*, Vol. 109, 187401, 2012.
57. He, J., P. Ding, J. Wang, et al., "Ultra-narrow band perfect absorbers based on plasmonic analog of electromagnetically induced absorption," *Optics Express*, Vol. 23, 6083–6091, 2015.
58. Bhattarai, M., V. Bharti, and V. Natarajan, "Tuning of the Hanle effect from EIT to EIA using spatially separated probe and control beams," *Scientific Reports*, Vol. 8, 7525, 2018.
59. Ning, R., Z. Jiao, and J. Bao, "Multi-band and wide-band electromagnetically induced transparency in graphene metasurface of composite structure," *IET Microwaves, Antennas & Propagation*, Vol. 12, 380–384, 2018.

60. Fan, Y., T. Qiao, F. Zhang, et al., "An electromagnetic modulator based on electrically controllable metamaterial analogue to electromagnetically induced transparency," *Scientific Reports*, Vol. 7, 40441, 2017.
61. Zhou, X., L. Zhang, A. M. Armani, et al., "Power enhancement and phase regimes in embedded microring resonators in analogy with electromagnetically induced transparency," *Optics Express*, Vol. 21, 20179–20186, 2013.
62. Wu, Y., J. Saldana, and Y. Zhu, "Large enhancement of four-wave mixing by suppression of photon absorption from electromagnetically induced transparency," *Physical Review A*, Vol. 67, 013811, 2003.
63. Tsakmakidis, K., M. Wartak, J. Cook, et al., "Negative-permeability electromagnetically induced transparent and magnetically active metamaterials," *Physical Review B*, Vol. 81, 195128, 2010.
64. Zhang, J., Z. Li, L. Shao, et al., "Active modulation of electromagnetically induced transparency analog in graphene-based microwave metamaterial," *Carbon*, Vol. 183, 850–857, 2021.
65. Zhang, L., P. Tassin, T. Koschny, et al., "Large group delay in a microwave metamaterial analog of electromagnetically induced transparency," *Applied Physics Letters*, Vol. 97, 241904, 2010.
66. Hu, Y., W. Liu, Y. Sun, et al., "Electromagnetically-induced-transparency-like phenomenon with resonant meta-atoms in a cavity," *Physical Review A*, Vol. 92, 053824, 2015.
67. Zhang, J., Y. Shi, and S. He, "Realizing flexible ultra-flat-band slow light in hybrid photonic crystal waveguides for efficient out-of-plane coupling," *Progress In Electromagnetics Research*, Vol. 149, 281–289, 2014.